Extraction of Coupling Coefficients of Directional Couplers Using Resonance Splitting

Ang Li, *Member, IEEE*, and Yeshaiahu Fainman, *Fellow, IEEE*

***Abstract*—We theoretically and experimentally present a novel method to accurately extract coupling coefficients of directional couplers using a single circuit. It utilizes the phenomenon of resonance splitting induced by mode coupling in a ring resonator, where the splitting distance is directly proportional to the coupling coefficient of the coupler that couples two modes. Compared with previous approaches, it doesn't rely upon measured amplitudes for parameter extraction, therefore, this method is insensitive to the uncertainties in the losses of other components in the circuit such as fiber/chip couplers, waveguides and resonators, as well as gage errors. More importantly, it can work with very weak coupling coefficients, down to 10^{-4}.**

***Index Terms*—Directional couplers, ring resonators, silicon photonics.**

I. Introduction

DIRECTIONAL couplers (DC) consisting of two parallel waveguides separated by a small gap are essential building blocks in integrated optics, due to its ability to split light with arbitrary ratios within a compact footprint compared with other splitters such as multi-mode interferometers (MMI), adiabatic mode converters, Y-junctions etc. [1], [2], [3]. On the other hand, their performance is very sensitive to the variation in physical parameters such as coupling gap and waveguide widths, which is a common issue of current fabrication technology, therefore, an accurate quantitative characterization of the performance of fabricated DCs, such as coupling coefficients, is critical for understanding and debugging the performance of the entire circuits consisting of these components.

Due to the non-negligible variation in the fiber/chip coupling losses and uncertainties in setup configuration when measuring different channels including fiber/chip misalignments, fibers distortions, setup vibration, gage errors etc., it's unreliable to extract the coupling coefficients of DCs by directly comparing the transmittance at its two output ports. A couple of more reliable approaches have been reported to extract coupling coefficients of DCs by using either a single ring resonator or unbalanced Mach-Zenhder-interferometers (MZI) [4], [5], [6]. In the transmission function of a single ring resonator, the coupling coefficient of the DC is mingled with the cavity loss as it is their product that impacts the transmission; thus they cannot be distinguished by analyzing a single resonance. The approach reported in [4] manages to extract the coupling coefficient from a single ring resonator by taking advantage of the dispersion effect of directional couplers, as the cavity loss is typically wavelength independent (even if it exhibits certain extent of fluctuations). By analyzing a series of resonances in a broad optical range can discern these two terms. Clearly, this condition limits the ability of this approach to extract coupling coefficients of broadband couplers that have much weaker wavelength dependency [7], [8], [9], [10]. Moreover, it cannot work with couplers with weak coupling coefficients, as the wavelength dependency of the coupler could be submerged by the stochastic variations of extracted cavity loss.

The approaches reported in [5], [6] incorporate DC in one or two MZIs and perform a multi-variable fitting of the transmittance of the MZIs to extract those parameters including coupling coefficients of the DC. This approach can only characterize couplers with strong coupling coefficients, as for weak couplers (<0.01), the significant imbalance in the two arms of an MZI would lead to transmission dips with very small extinction ratios, seriously decreases the accuracy. Also, for the approaches introduced above, they are still faced the problem of uncertainty in measurement setup and variation in fiber couplers as they are processing absolute measured power.

In this paper, we propose and experimentally demonstrate a novel method to extract coupling coefficient of a directional coupler, or any kind of 4-port couplers such as multi-mode-interferometer (MMI). The method utilizes the phenomenon of resonance splitting between two coupled resonant modes as the splitting distance is directly dependent on the field coupling coefficient κ_{dc} of the coupler that couples two modes. This phenomenon has been previously used in other applications [11]. It only needs to measure the transmission spectrum of a single channel and obtains information from the resonance locations instead of absolute amplitude transmission, thus is insensitive to fiber couplers variations and measurement setup uncertainty. Based on the configurations, the resonance splitting between two modes coupled by the to-be-characterized 4-port coupler (denoted with DUT) can be either two modes from two separate

Manuscript received 6 November 2022; accepted 9 November 2022. Date of publication 11 November 2022; date of current version 24 November 2022. This work was supported in part by National Key R&D Program of China under Grant 2021YFB2801500, in part by the Distinguished Professor Fund of Jiangsu Province, Fundamental Research Funds for the Central Universities under Grant NS2022043, in part by the National Natural Science Foundation of China under Grant 62105149, and in part by the Natural Science Foundation of Jiangsu Province under Grant BK20210288. *(Corresponding author: Ang Li.)*

Ang Li is with the Key Laboratory of Radar Imaging and Microwave Photonics, Ministry of Education, Nanjing University of Aeronautics and Astronautics, Nanjing 210016, China (e-mail: ang.li@nuaa.edu.cn).

Yeshaiahu Fainman is with the Department of Electrical and Computer Engineering, University of California at San Diego, La Jolla, CA 92093 USA (e-mail: fainman@ee.ucsd.edu).

Digital Object Identifier 10.1109/JPHOT.2022.3221487

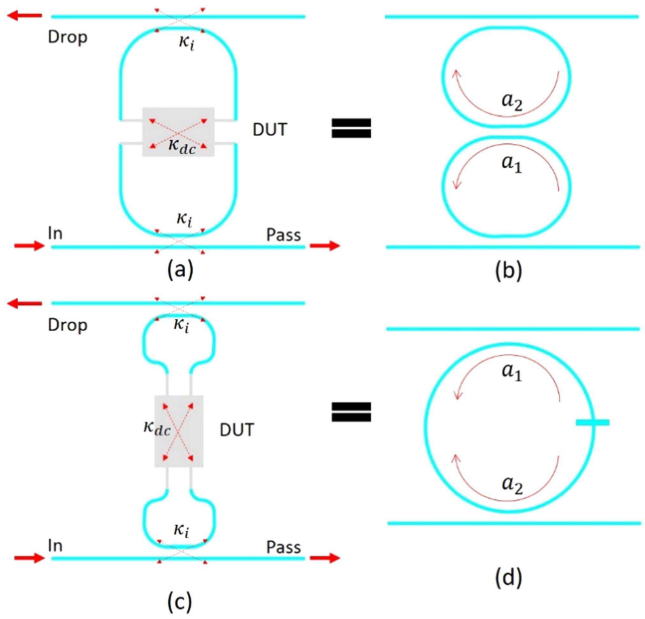

Fig. 1. Two different configurations to get two resonant modes coupled by the 4-port device under test (DUT). The two modes can be from two separate resonators (a-b) or two originally degenerate modes in a single resonator.

resonators (Fig. 1(a)-(b)) or two originally degenerate modes in a single resonator (Fig. 1(c)-(d)). Correspondingly, the DUT is embedded into either a coupled-resonator system or a single resonator. In this work, we chose to embed it into a single resonator as in such a circuit, the two modes are inherently identical, while the fabrication variation might cause the two modes in a coupled-resonator system to be slightly different in terms of resonant frequency and decay rate. Besides, this configuration gives another advantage in terms of accuracy and working range, as for each roundtrip length, the two modes coupled twice through this coupler while for the structure in Fig. 1(a)-(b), two modes only couple once per roundtrip travelling. Consequently, the same coupling coefficient can lead to a larger and clearer resonance splitting.

According to temporal Coupled-Mode-Theory (tCMT) [12], [13], the mode equations for circuit shown in Fig. 1(c)-(d) can be formulated in the following way:

$$\frac{da_1}{dt} = j\left(\omega_0 + j\frac{1}{\tau_{tot}}\right)a_1 - j\mu_{dc}a_2 - j\mu_i S_i \tag{1}$$

$$\frac{da_2}{dt} = j\left(\omega_0 + j\frac{1}{\tau_{tot}}\right)a_2 - j\mu_{dc}a_1 - j\mu_i' S_i \tag{2}$$

where $a_1,\ a_2$ refers to the amplitudes of the two modes in the resonator, respectively. They are normalized in such a way that their squares represent the total energy stored in these modes. ω_0 is the resonant frequency of the two modes, which is purely determined by the physical parameters of the resonators such as roundtrip length L and waveguide index. In this case, the two modes have identical resonant frequencies. $\frac{1}{\tau_{tot}}$ is the total decay rate of each mode, covering contributions from waveguide loss $\frac{1}{\tau_\alpha}$ and coupling to two external waveguides $2 * \frac{1}{\tau_i}$ ($\frac{1}{\tau_{tot}} = \frac{1}{\tau_\alpha} + \frac{2}{\tau_i}$). Note that the two couplers of the resonators are designed to be identical. Decay rate $\frac{1}{\tau_{tot}}$ describes how fast the energy inside the cavity decays in time domain, and it is related with the field loss factor α by taking the circulating time into account:

$$\frac{2}{\tau_\alpha} = \alpha^2\ \frac{v_g}{L} = \alpha^2\ \frac{c}{n_g L} \tag{3}$$

where v_g is the group velocity, c is light speed in vacuum and n_g is the group index of the ring waveguide. $n_g L$ can be determined by measuring the free-spectral-range (FSR) as $n_g L\ = \frac{\lambda_0^2}{FSR}$.

μ_i stands for the coupling from input signal S_i to resonant mode a_1. Similarly, μ_i' refers to the coupling from input wave to resonant mode a_2, which is named as backcoupling, which is the coupling from external input to the reversely circulating mode. For ideal direction couplers, it is 0, while in reality, there can exist a small amount of backcoupling depending on the couplers' geometry. More details about the backcoupling can be found in [14]. μ_{dc} is the so-called mutual coupling term that couples the two resonant modes through the DUT to be characterized. Similar to decay rate $\frac{1}{\tau_i}$, μ_i and μ_{dc} in tCMT are terms in time domain and are also connected with the physical parameters through following equations [12], [13]:

$$\mu_i^2 = \frac{2}{\tau_i}\ = \kappa_i^2\ \frac{v_g}{L} = \kappa_i^2\ \frac{c}{n_g L} \tag{4}$$

$$\mu_{dc} = \ 2\kappa_{dc}\ \frac{v_g}{L} = \ 2\kappa_{dc}\frac{c}{n_g L} \tag{5}$$

Where κ_i refers to the field coupling coefficient of the ring couplers, as shown in Fig. 1(a). The factor 2 on the right side of (5) is simply due to the fact that for each roundtrip, the two modes couple twice, which is slightly different for the structure in Fig. 1(d), where they are coupled by a lumped element once per roundtrip travelling. The transmission at pass port and drop port are governed by (6)-(7):

$$S_t = S_i\ - j\mu_i a_1 - j\mu_i' a_2 \tag{6}$$

$$S_d = \ -j\mu_i a_2 - j\mu_i' a_1 \tag{7}$$

For the following content, we only analyze the drop port transmission, but all the theories work for pass port as well. Solving (1)-(2) at steady state could produce quantitative expression of mode amplitudes of a_1 and a_2 (time dependency exp(−jωt) is omitted for simplicity), substituting them into (6) yields the final equation for the transmission at drop port as (8):

$$\frac{S_d}{S_i} = \left(\frac{(1-f)^2/\tau_i}{j\,(\omega-\omega_1) + 1/\tau_{tot}}\right) + \left(\frac{(1+f)^2/\tau_i}{j\,(\omega-\omega_2) + 1/\tau_{tot}}\right) \tag{8}$$

$$\omega_1 = \omega_0\ - \mu_{dc},\quad \omega_2 = \omega_0\ + \mu_{dc} \tag{9}$$

Here, f is a dimensionless factor connecting backcoupling μ_i' and forward coupling μ_i: $\mu_i' = \ f\mu_i$. By doing so, we can arrive at a clearer mathematical expression to better analyze the transmission. Clearly, due to the presence of mutual coupling term μ_{dc}, the transmission shows a resonance splitting, whose distance in frequency domain directly depends on the mutual coupling term ($\Delta\omega\ =\ 2\mu_{dc}$), thus the field coupling coefficient κ_{dc}. Note

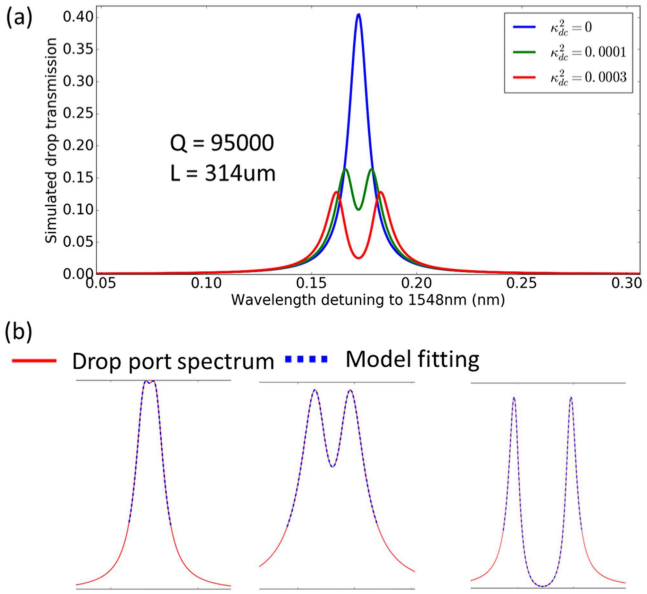

Fig. 2. A tiny amount coupling for structure in Fig. 1(c) can lead to clearly visible resonance splitting (a) and (b) shows the fitting quality of (7). The x axis is wavelength and y axis refers the power transmission in linear scale.

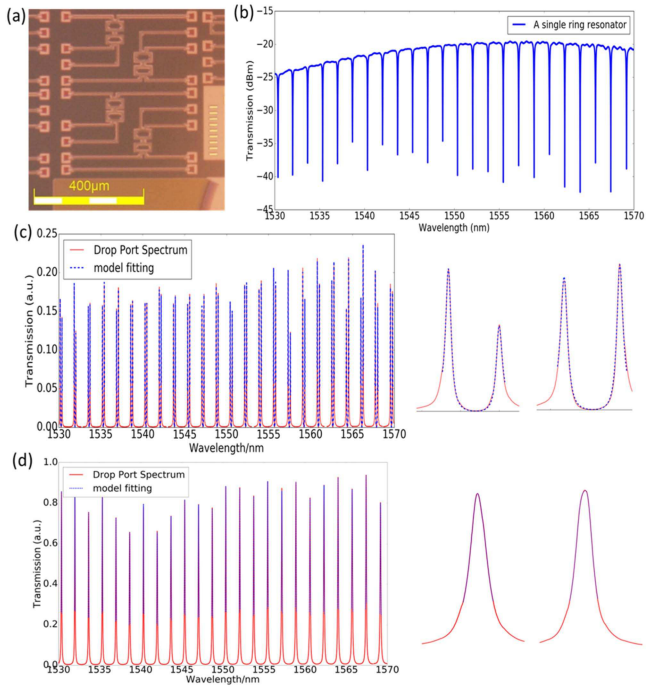

Fig. 3. (a) Gives the microscopic image of the fabricated devices. (b) presents the measured spectrum of a standing-alone ring resonator as reference, to confirm the absence of backscattering induced resonance splitting. (c-d) plot the measured spectrum and fitting results using (8) of two devices with DUTs that have coupling coefficients of 0.15 and 0.001 respectively.

that backcoupling only affects the amplitude of individual peak and doesn't contribute to the splitting distance. Obviously, our approach doesn't require absolute value of measured intensity, instead, only spectral features such as splitting distance, FSR and central wavelength are required. And those parameters can be obtained by fitting a measured transmission spectrum using (8). Therefore, it is very robust to fabrication variation on auxiliary components like grating couplers which might introduce uncertainty in the total power transmission. Once those parameters are obtained, the exact amount of coupling coefficient of DUT can be calculated using (5). For resonator with high Q factor, a tiny amount of coupling can lead to a clearly visible resonance splitting as evident in Fig. 2(a). Therefore, this method can work with very weak coupling coefficients.

We first use optical circuit simulator Caphe [15] to test the performance of the method. In the simulator, each ring resonator has a length of 314um with waveguide loss of 2 dB/cm. The Q factor of the resonance is about 100000. For simplicity, in the circuit model, the couplers do not introduce backcoupling, therefore, the split resonances are always symmetric in terms of peak amplitudes. We use (8) to fit the transmission spectrum and calculate the coupling coefficient κ_{dc}, then compare with the setting values in Caphe. The fitting quality for various splitting conditions is given in Fig. 2(b) and the numerical results are given in Table 1. Note that, the initial values of the parameters for fitting multiple variables are crucial for the overall fitting performance, especially when working with relatively less advanced algorithms. Our code is developed in such a way that the initial values of the to-be-fit parameters such as resonant wavelength, FSR, decay rate $\frac{1}{\tau_{tot}}$, mutual coupling term μ_{dc} are all automatically derived from the input data with high confidence. Therefore, even resonances with almost invisible splitting can be accurately fitted. Thanks to this, coupling coefficients down to $0.5 * 10^{-4}$ can be accurately extracted with Q factor around 100000, which is achievable for silicon ring resonator, as Q factor as high as 400000 has been reported [16].

TABLE 1
SIMULATED RESULTS USING CAPHE TO CALIBRATE THE PERFORMANCE OF THE METHOD

Setting value κ_{dc}^2	Slitting distance (pm)	Calculated κ_{dc}^2
5e-5	7.86	4.99e-05
1e-4	11.1	9.98e-05
0.001	35.15	0.0009983
0.01	111.33	0.010013
0.1	357.6	0.10331432

The devices were fabricated at Applied Nanotools using Electron beam lithography on a 220 nm thick silicon on insulator wafer. All the waveguides are strip waveguides. Additional oxide cladding is deposited on top of silicon layer. Grating couplers are used as fiber/chip interfaces. The couplers of the ring resonators are designed to work at critical coupling condition. In order to reduce the backscattering induced by waveguide sidewall roughness, which is detrimental for the Q factor and might also cause stochastic resonance splitting [12], the straight sections of the ring cavity are broadened to 1 um while the bending sections are 500 nm wide single mode waveguide with spline shape, which are believed to introduce negligible loss and reflections. Adiabatic tapers are employed to connect 1um and 500 nm waveguide without activating higher order modes.

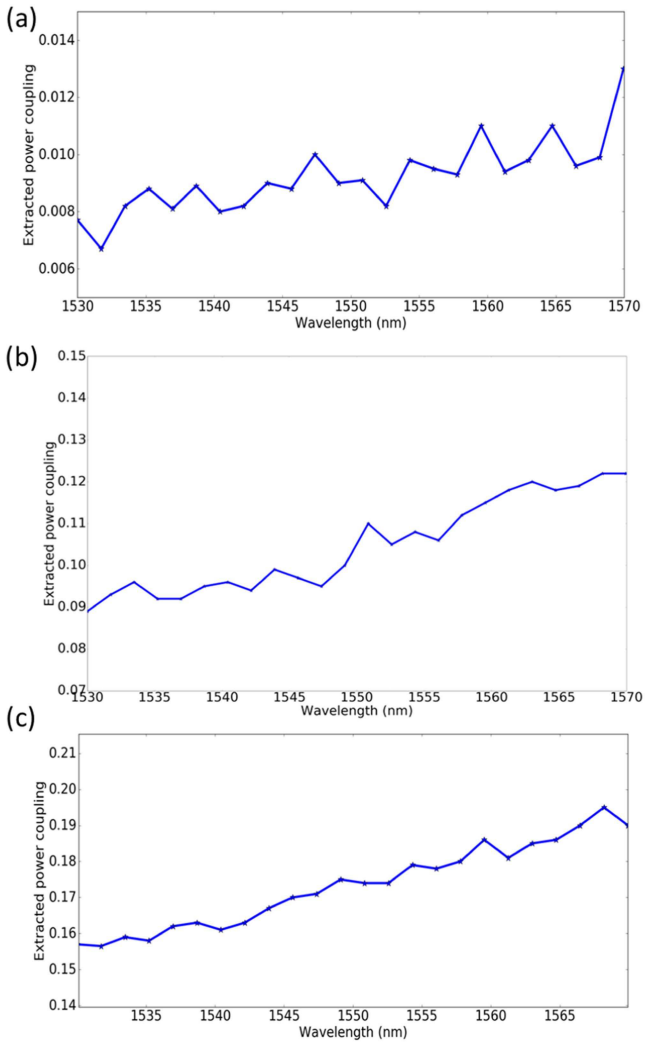

Fig. 4. (a-c) Plot the extracted power coupling coefficients of two direction couplers with simulated κ_dc^2 around 0.005, 0.1 and 0.15 respectively.

Silicon ring resonators with this kind of hybrid waveguide to reduce cavity loss have been reported to produce Q factor over 1 million [16], [17]. The microscopic image of the devices is given in Fig. 3(a). We fabricated devices with 4 different coupling coefficients, which are 0.001, 0.005, 0.1 and 0.15 (simulated values) at 1550nm, respectively. To confirm the absence of backscattering induced splitting in the ring resonator, a reference ring resonator with the same design and physical parameters is also fabricated. The measured transmission spectrum is given in Fig. 3(b), The measured Q factor is about 70000 and no visible splitting is observed which indicates negligible backscattering. Therefore, any kind of resonance splitting would be induced by the directional couplers inside the rings.

The exemplar measured spectrum and fitting results are given in Fig. 3(b). As explained above, the asymmetry in the peak amplitudes of the split resonance is due to the parasitic back-coupling of the couplers, but it doesn't contribute to the splitting distance, which is purely dependent on the power coupling coefficient of the embedded couplers (DUT). For those devices under test, the device with 0.001 coupling coefficient doesn't exhibit any visible resonance splitting as shown in Fig. 3(d), therefore the results are less reliable. The reason is that the current resonances with Q factor of 70000 are too broad to resolve the splitting induced by the coupling coefficient of 0.001. Simulations shown in Fig. 2 suggest that a resonance with Q factor around 90000 is required to show visible splitting caused by coupling coefficient down to 0.001. The extracted power coupling coefficients of the other 3 (0.005, 0.1 and 0.15) couplers are presented in Fig. 4. The discrepancy between the extracted values and simulated values can be attributed to fabrication variation in the waveguide widths as well as the gap between two waveguides. The etching process would typically lead to angled waveguide sidewalls, effectively reducing the gap between two waveguides, therefore leading to higher coupling coefficients than simulated values. While the fluctuation in each curve is due to residual parasitic reflections inside the ring resonators and fitting errors that serve as noise to the extracted values. This effect is weaker for stronger coupling coefficient with clearer resonance splitting as evident in Fig. 4(b)–(c).

In conclusion, we propose and experimentally demonstrate a new method to extract coupling coefficients of directional couplers, which is based on resonance splitting of coupled modes. Compared with previous approaches, it does not rely upon accurate power measurements and can work well with weak coupling coefficients. Simulation results show that it can work with power coupling coefficients down to 10^{-4} with a Q factor over 90000. The circuit proposed in this work can serve as a good test structure to characterize fabricated direction couplers, or any 4-port couplers.

Disclosures

The authors declare no conflicts of interest.

References

[1] A. Melikyan and P. Dong, "Adiabatic mode converters for silicon photonics: Power and polarization broadband manipulators," *APL Photon.*, vol. 4, 2019, Art. no. 030803.
[2] D. Thomson, Y. Hu, G. Reed, and J.-M. Fedeli, "Low loss MMI couplers for high performance MZI modulators," *IEEE Photon. Technol. Lett.*, vol. 22, no. 20, pp. 1485–1487, Oct. 2010.
[3] Y. Zhang et al., "A compact and low loss Y-junction for submicron silicon waveguide," *Opt. Exp.*, vol. 21, pp. 1310–1316, 2013.
[4] W. McKinnon et al., "Extracting coupling and loss coefficients from a ring resonator," *Opt. Exp.*, vol. 17, pp. 18971–18982, 2009.
[5] Y. Xing, J. Dong, S. Dwivedi, U. Khan, and W. Bogaerts, "Accurate extraction of fabricated geometry using optical measurement," *Photon. Res.*, vol. 6, pp. 1008–1020, 2018.
[6] M. A. Tran, T. Komljenovic, J. C. Hulme, M. L. Davenport, and J. E. Bowers, "A robust method for characterization of optical waveguides and couplers," *IEEE Photon. Technol. Lett.*, vol. 28, no. 14, pp. 1517–1520, Jul. 2016.
[7] G. F. Chen, J. R. Ong, T. Y. Ang, S. T. Lim, C. E. Png, and D. T. Tan, "Broadband silicon-on-insulator directional couplers using a combination of straight and curved waveguide sections," *Sci. Rep.*, vol. 7, pp. 1–8, 2017.
[8] S. Nevlacsil et al., "Broadband SiN asymmetric directional coupler for 840 nm operation," *OSA Continuum*, vol. 1, pp. 1324–1331, 2018.
[9] R. Halir et al., "Colorless directional coupler with dispersion engineered sub-wavelength structure," *Opt. Exp.*, vol. 20, pp. 13470–13477, 2012.
[10] R. K. Gupta, S. Chandran, and B. K. Das, "Wavelength-independent directional couplers for integrated silicon photonics," *J. Lightw. Technol.*, vol. 35, no. 22, pp. 4916–4923, Nov. 2017.

[11] M. Bayer et al., "Optical modes in photonic molecules," *Phys. Rev. Lett.*, vol. 81, pp. 2582–2585, 1998.
[12] A. Li, T. Van Vaerenbergh, P. De Heyn, P. Bienstman, and W. Bogaerts, "Backscattering in silicon microring resonators: A quantitative analysis," *Laser Photon. Rev.*, vol. 10, pp. 420–431, 2016.
[13] Q. Li, T. Wang, Y. Su, M. Yan, and M. Qiu, "Coupled mode theory analysis of mode-splitting in coupled cavity system," *Opt. Exp.*, vol. 18, pp. 8367–8382, 2010.
[14] A. Li and W. Bogaerts, "Using backscattering and backcoupling in silicon ring resonators as a new degree of design freedom," *Laser Photon. Rev.*, vol. 13, 2019, Art. no. 1800244.
[15] M. Fiers et al., "Time-domain and frequency-domain modeling of nonlinear optical components at the circuit-level using a node-based approach," *JOSA B*, vol. 29, pp. 896–900, 2012.
[16] M. Burla, B. Crockett, L. Chrostowski, and J. Azaña, "Ultra-high Q multimode waveguide ring resonators for microwave photonics signal processing," in *Proc. Int. Topical Meeting Microw. Photon.*, 2015, pp. 1–4.
[17] H. Qiu et al., "A continuously tunable sub-gigahertz microwave photonic bandpass filter based on an ultra-high-Q silicon microring resonator," *J. Lightw. Technol.*, vol. 36, no. 19, pp. 4312–4318, Oct. 2018.